RESEARCH ARTICLE

Removal of Pb(II) Ion by Iron Oxide Nanoparticles Prepared by Annealing at Two Different Temperatures

Aliakbar Dehno Khalaji[1,]*, Marketa Jarosova[2], Pavel Machek[2] and Michal Dusek[2]

[1]*Department of Chemistry, Faculty of Science, Golestan University, Gorgan, Iran.*

[2]*Institute of Physic of the Czech Academy of Sciences, v.v.i., Na Slovance 2, 182 21 Prague 8, Czech Republic.*

ARTICLE INFO

Article History:
Received 2021-06-06
Accepted 2021-09-26
Published 2022-03-01

Keywords:
Nanoparticles
Fe_2O_3
Calcination
Pb(II) adsorption
Removal

ABSTRACT

Transition metal ions have been extensively studied for the removal of heavy metal ions as efficient adsorbent from aqueous solution. In this work, Fe_2O_3 nanoparticles were synthesized by thermal decomposition route of $FeSO_4{\cdot}4H_2O$ in the presence of urea (1:1 molar ratio) at two different temperatures (500 °C and 600 °C) and characterized by XRD and TEM. The XRD result shows that single-phase of α-Fe_2O_3 was prepared by increasing of calcination temperature from 500 °C to 600 °C. TEM images confirmed that the as-prepared products have a different shape and that particle sizes are in the range of tens nanometers. The average crystallite size of pure α-Fe_2O_3 calculated from the XRD pattern was 53.1 nm and 41 nm, respectively, depending on the method employed. In addition, Pb(II) adsorption has been studied and considered as a function of pH solution, contact time, initial Pb(II) concentration and also adsorbent dosage. The adsorption results show that the iron oxides were able to high percentage remove Pb(II) by increasing of contact time, adsorbent dosage and initial Pb(II) ion. The pH solution of 6 proved to be the most suitable for the removal of Pb(II).

How to cite this article
Dehno Khalaji A., Jarosova M., Machek P., Dusek M. Removal of Pb(II) Ion by Iron Oxide Nanoparticles Prepared by Annealing at Two Different Temperatures. J. Nanoanalysis., 2022; 9(1): 83-89. DOI: 10.22034/jna.2021.1932617.1258.

INTRODUCTION

Nowadays, water is one of the most important natural resources due to its usability for various human and plant activities [1]. In recent years, access to safe drinking water became very limited, due to an increased discharge of various industrial wastewaters containing harmful and toxic transition metal ions or azo organic dyes to the environment [2-5]. Heavy metal ions [4, 5] and organic dyes [2,3] were characterized by their high stability and can remain in the environment for a long time. Therefore, eliminating or destroying these polluting factors from the environment is one of the main challenges that human society faces [2-5]. Lead, mercury and cadmium ions belong to the most toxic metal ions. Their contamination in the human body causes diseases of the liver, lungs, brain and eventually death. The World Health Organization has set the minimum amount of these ions in drinking water between 0.01 and 0.005 mg/L. So far, many methods have been used to remove heavy metal ions [4-17]. Among all the methods, the adsorption method has received the most attention of research groups due to its simplicity, cheapness, sensitivity and high efficiency for the removal of various metal ions [4-9]. One of the important parameters in the efficiency of this method is the type of adsorbent used such as activated bentonite [18,19], modified lignin hydrogel [20], zinc oxide/graphene oxide composite [21], xanthation-modified deoiled allspice husk [22], sheep wool [23], mesoporous silica MCM-41 modified by $ZnCl_2$ [24], barium/cobalt@polyethylene glycol nanocomposites [25], micro-spheres of *Zea mays* rachis–sodium alginate [26], *penicillium polonicum* [27], Fe_2O_3@SiO_2 nanocomposite [28]. Ahmad and Mirza [4] reported the chitosan iron oxide nanocomposite as new adsorbent to removal of lead and cadmium ions. Li *et al.* [6] studied the removal

* Corresponding Author Email: *alidkhalaji@yahoo.com*

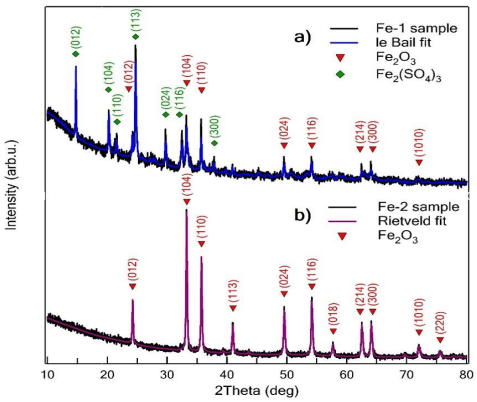

Fig. 1. The XRD patterns of iron oxide nanoparticles a) Fe-1 and b) Fe-2.

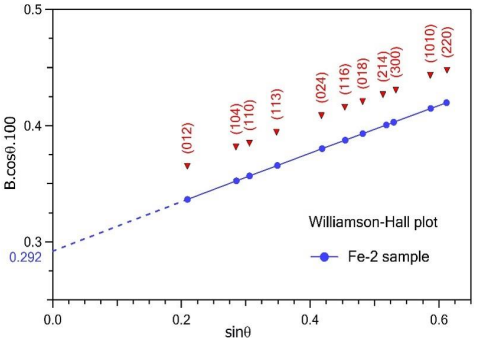

Fig. 2. Williamson-Hall plot of iron oxide nanoparticles Fe-2.

of lead and cadmium ions by modified chitosan by thiosomalcarbazide. Hematite nanoparticles as adsorbents used to remove lead, cadmium, copper and zinc ions by Shipley *et al.* [7]. Van Tran *et al.* [8] applied new two-binary Cu-Mg ferrite nanoparticles to remove lead ions. Kumar Raul *et al.* [5] reported the removal of lead ion using copper oxide nanoparticles. Homayonfard *et al.* [9] used chitosan ferrite nanocomposite to remove cadmium ion from aqueous medium.

In recent years, Fe_2O_3 nanoparticles have been used as well adsorbent for removal of heavy metal ions and various organic dyes due to excellent adsorption capacities [7, 29-36]. Fe_2O_3 nanoparticles, the most stable iron oxide, low-cost materials, easily removed using a magnet and environmental friendly, with large surface area have the high active sites to adsorb heavy metal ions or organic dyes [29-36].

Continuing the previous work on the preparation of various transition metal nanoparticles [37-41], in this study, iron oxide nanoparticles were prepared by solid state thermal degradation of a mixture of ferrous sulfate and urea at temperatures of 500 and 600 °C and characterized using XRD and TEM. In addition, the removal of lead ion from aqueous solution was studied by changing parameters such as solution pH, contact time, lead ion concentration and amount of adsorbent dosage.

EXPERIMENTAL

Materials and measurement

All chemicals used in this paper, such as $FeSO_4.4H_2O$, urea, $Pb(NO_3)_2.2H_2O$ and HCl, were purchased from a Merck company and were used without any further purification. XRD patterns of the complexes were obtained on Empyrean powder diffractometer of PANalytical in Bragg-Brentano configuration equipped with a flat sample holder and PIXCel3D detector (Cu Kα radiation, λ = 1.5418 Å). Particle images were recorded with a transmission electron microscope (TEM) FEI Tecnai G^2 20 with a LaB_6 cathode at acceleration voltage 200 kV. The instrument is equipped with a CCD camera Olympus Veleta. The Pb(II) ion analysis was carried out by Atomic Absorption spectrophotometer (Shimadzu AA-6300, Japan).

Preparation of iron oxide nanoparticles

α-Fe_2O_3 nanoparticles prepared using solid-

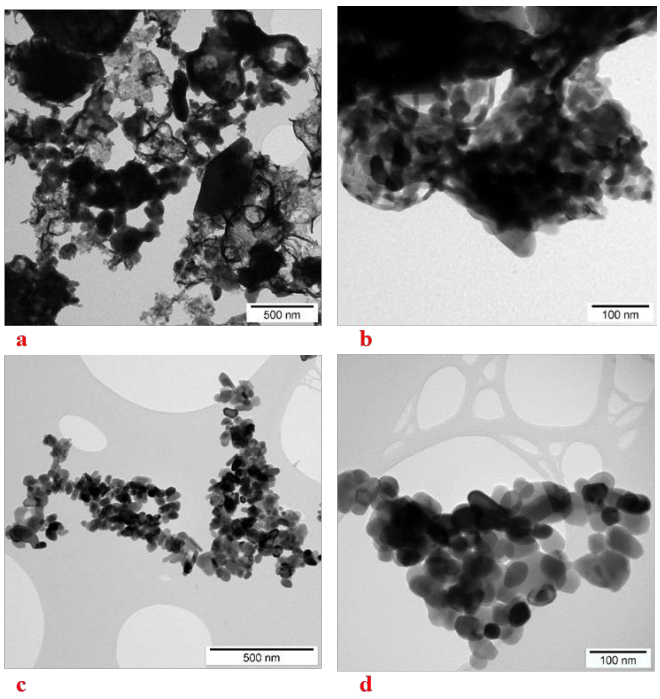

Fig. 3. TEM images of a,b) Fe-1 and c,d) Fe-2.

state thermal decomposition according to the previous literature [37,38,42]. $FeSO_4.4H_2O$ (0.01 mol) and urea (0.01 mol) were mixed into a quartz crucible and ground for about 10 min. Finally, the powder was put into a tube furnace and calcined for 2 h at 500 °C and 600 °C with a heating rate of 20 °C/min under air atmosphere. As a result, two products were obtained and respectively named as Fe-1 and Fe-2.

Adsorption experiments

Pb(II) ion removal experiments were performed in 50 ml Erlenmeyer flask containing 25 ml of lead solution at different concentrations, in the presence of different amounts of adsorbent at different times and at different pH of the solution. The flasks were then shaken, and at various contact times, the adsorbent was separated from the solution using a centrifuge. Then, Pb(II) concentration was recorded by using atomic absorption spectrophotometer. The removal percentage (%) and the amount of adsorbed per unit mass of adsorbent (mg/g) were obtained using the equations bellow:

$$R\ (\%) = \{(C_i - C_t) / C_i\} \times 100 \qquad (1)$$

$$q_t = \{(C_i - C_t)\ V\} / M$$

where, R (%) is the removal percentage, q_t (mg/g) is the adsorption capacity, C_i and C_t are initial and final Pb(II) concentrations, V (L) is the volume of the solution and M (g) is the adsorbent dosage.

RESULTS AND DISCUSSION

XRD patterns

The XRD patterns of the Fe-1 and Fe-2 products are presented in Fig. 1. It appeared that sample Fe-1 is a mixture of Fe_2O_3 and $Fe_2(SO_4)_3$, both rhombohedral, and of a small amount of the other compound which cannot be identified unambiguously. By increasing the annealing temperature from 500 °C to 600 °C, the intermediate products have been disappeared and pure α-Fe_2O_3 nanoparticles were obtained. In the XRD pattern of Fe-2, 11 sharp diffraction peaks at 2θ ≈ 24.14°(012), 33.14°(104), 35.62°(110), 40.85°(113), 49.44°(024), 54.04°(116), 57.56°(018), 62.41°(214), 63.98°(300), 71.89°(1010) and 75.43°(220) are observed. These diffraction peaks can be indexed to the hexagonal phase of α-Fe_2O_3 with card JCPDS No. 80-2377 [30-32].

The rhombohedral structure of the product was confirmed by the Rietveld fit in crystallographic program Jana2006 [43] with calculated lattice constants of a=5.0365(2) Å and c= 13.7586(7) Å which are in good agreement with the tabulated

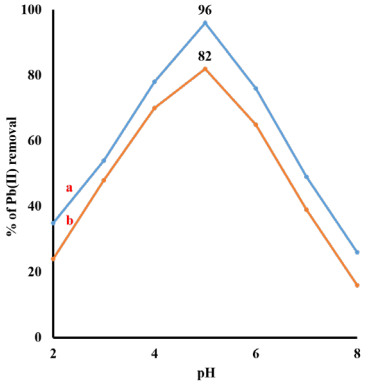

Fig. 4. Effect of pH on adsorption of Pb(II) on (a) Fe-2 and (b) Fe-1 (0.4 g adsorbent with 25 mL of 50 ppm initial concentration of Pb(II) at 120 min).

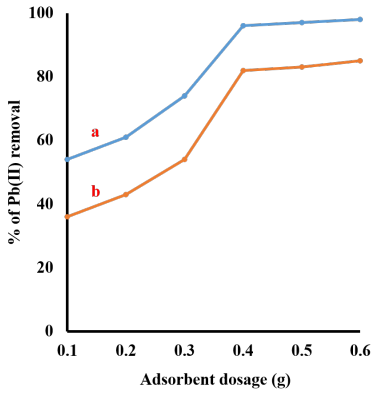

Fig. 5. Effect of adsorbent dosage on adsorption of Pb(II) on (a) Fe-2 and (b) Fe-1 (25 mL of 50 ppm initial concentration of Pb(II) at 120 min and pH = 5).

values. The average crystallite size was determined using both Williamson-Hall analysis [44] and fundamental parameter approach [45]. In the first case, the diffraction pattern of NIST standard LaB_6 collected under the same conditions as Fe-2 sample was employed as instrumental function. The distinct dependencies of size and strain broadening on the diffraction angle allowed separating both effects in Williamson-Hall plot (Fig. 2):

$$\beta \cos\theta = k.\frac{\lambda}{L} + 4\varepsilon.\sin\theta \qquad (2)$$

Where β is peak width, θ diffraction angle, k is a constant which depends on the assumptions made in the theory, λ is wavelength of the radiation, L is average crystallite size and ε is strain [46]. In the presented case, we assumed that strain is uniform and Scherrer constant equals 1. By fitting the data, average crystallite sizes were extracted from the y-intercepts. For the sample Fe-2 we obtained intercept K1=0.292 resulting in average crystallite size 53.1 nm.

In the other case, the instrumental function was modeled from the known geometry of the diffractometer and from the predefined radiation profiles. The instrumental broadening b_{inst} was subsequently extracted from the measured diffraction pattern and sample broadening b_{sample} was determined. Average crystallite size of sample Fe-2 was then solved using Scherrer equations

$$D_v = K\,\lambda\,/\,(\beta_{sample}\cos\theta) \qquad (3)$$

where D_v is volume weighted crystallite size, K is Scherrer constant, l wavelength of the radiation and b_{sample} is integral breadth of reflection located at angle 2q. The average crystallite size determined for the as-prepared product at 600 °C is 41 nm.

TEM images

The TEM imaging was carried out to determine the morphology and particle size. The sample prepared at 500 °C contained semi-elliptical particles and any residual matter (Fig. 3a). Because of iron oxide particles make clusters, the particle size can be only roughly estimated to tens of nanometers (Fig. 3b). Iron oxides prepared by calcination at 600 °C also make clusters. Nevertheless, the individual particles are simply recognized (Fig. 3c,d). The spherical nanoparticles with a diameter of about 30-65 nm and elongated particles with a longer diameter up to 100 nm were found in this sample.

Effect of pH on adsorption

The effect of pH values on the Pb(II) adsorption using the as-prepared iron oxides Fe-1 and Fe-2 were investigated and the data are shown in Fig. 4. Fig. 4 shows that in all pH the efficiency of Pb(II) ion adsorption by Fe-2 as adsorbent is higher than Fe-1. In addition, at lower pH, Pb(II) ion adsorption efficiencies are low, due to the high concentration of H^+ ions. Because H^+ ion is lighter than Pb(II) ion, it can be more easily adsorbed on the adsorbent surface. Therefore, the H^+ ion wins the competition with the Pb(II) ion. In other words, the active sites of the adsorbent to absorb the Pb(II) ion are blocked by the H^+ ions [51-53]. Also, with increasing pH and decreasing the H^+ concentration, Pb(II) ion can be adsorbed by high-level activity of nanoparticles and it is observed that by increasing the pH and going from 2 to 5, the adsorption efficiency of Pb(II) ion reaches from

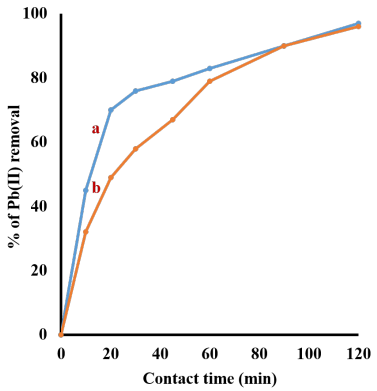

Fig. 6. Effect of initial Pb(II) concentration (a) 30 and (b) 50 ppm on adsorption of Pb(II) on Fe-1.

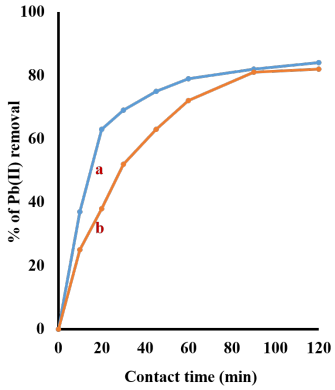

Fig. 7. Effect of initial Pb(II) concentration (a) 30 and (b) 50 ppm on adsorption of Pb(II) on Fe-2.

25% to 96% on Fe-2 and 24% to 82% on Fe-1 [6, 8, 47-52].

As the pH increases and the solution reaches a neutral or alkaline pH, it is observed that the Pb(II) ion removal efficiency decreases. Under these conditions, Pb(II) ions in the presence of hydroxide ions can easily produce $Pb(OH)_2$, $PbOH^+$ and also $Pb(OH)_3^-$ [6, 8, 47-52], which is stable and cannot be absorbed by the adsorbent and removed from the aqueous solution. Then, according to the obtained results, pH 5 was selected to continue the experimental work and to investigate the effect of contact time, change of lead ion concentration and change of adsorbent amount.

Effect of adsorbent dosage

The metal ion removal efficiency is directly related to the amount of adsorbent used. By changing the amount of adsorbent due to the change in the amount of active groups in adsorption as well as electrostatic interactions with metal ions, the amount of metal ions removed from the solution increases. Fig. 5 shows the effect of different amounts of adsorbents used in the removal of lead ions for the two adsorbents Fe-1 and Fe-2. Fig. 5 shows that by increasing the amount of adsorbent from 0.1 g to 0.4 g, the Pb(II) ion removal efficiency has increased from 54 to 96% for Fe-2 and 36 to 82% for Fe-1. These changes are due to the increase in the amount of active adsorption groups when higher amounts of adsorbent are used [12, 47-52]. In addition, Fig. 5 shows that further use of adsorbent (0.5 and 0.6 g) has little effect on lead ion uptake.

Effect of initial Pb(II) concentration and contact time

Adsorption of Pb(II) by the adsorbent is directly related to its initial concentration in solution. The results of Pb(II) ion removal with changes in its initial concentration in solution from 30 to 50 ppm are shown in Figs. 6 and 7, respectively. These figures show that the time to reach the maximum amount of Pb(II) ion removal in the initial concentration of 30 ppm is shorter than the concentration of 50 ppm [48,49]. Due to the greater number of active adsorbent sites for adsorption at low concentration of Pb(II) ion, the adsorption rate is higher and in less time the maximum amount of Pb(II) ion adsorption occurs on the adsorbent surface. By increasing the initial concentration of Pb(II) ions, the active adsorption sites are saturated sooner, so the time to reach the maximum amount of adsorption is longer.

CONCLUSIONS

New iron oxides (Fe-1 and Fe-2) were prepared and characterized. XRD results show that the Fe-1 is mixture of α-Fe_2O_3 nanoparticles and intermediate products, while Fe-2 is rhombohedral structure of pure α-Fe_2O_3. TEM images show the semi-elliptical particles with a size of tens of nanometers. In addition, the Pb(II) removal of the as-prepared iron oxide products has been studied. Adsorption results show that with increasing the pH solution, adsorbent dosage and also contact time, the percentage removal of Pb(II) has been increased.

ACKNOWLEDGMENTS

We would like to thank the Golestan University and Institute of Physic of the Czech Academy of Sciences for financial their supports. The work is supported by Operational Programme Research, Development and Education financed by European Structural and Investment Funds and the Czech

Ministry of Education, Youth and Sports (Project No. SOLID21 CZ.02.1.01/0.0/0.0/16_019/0000760).

CONFLICT OF INTEREST

The authors declare that there is no conflict of interest.

REFERENCES

1. Natarajan, S., Bajaj, H.C., Tayade, R.J., J. Environment. Sci. 201, 201-222 (2018) https://doi.org/10.1016/j.jes.2017.03.011
2. Saha, B., Das, S., Saikia, J., Das, G., J. Phys. Chem. C. 115, 8024-8033 (2011) https://doi.org/10.1021/jp109258f
3. Ye, C., Hu, K., Niu, Z., Lu, Y., Zhang, L., Yan, K., J. Water Process. 27, 205-210 (2019) https://doi.org/10.1016/j.jwpe.2018.12.008
4. Ahmad, R., Mirza, A., J. Clean. Product. 186, 342-352 (2018) https://doi.org/10.1016/j.jclepro.2018.03.075
5. Kumar Raul, P., Senapati, S., Sahoo, A.K., Umlong, I.M., Devi, R.R., Thakur, A.J., Veer, V., RSC Adv. 4, 40580-40587 (2014) https://doi.org/10.1039/C4RA04619F
6. Li, M., Zhang, Z., Li, R., Wang, J.J., Ali, A., Int. J. Biol. Macromol. 86, 876-884 (2016) https://doi.org/10.1016/j.ijbiomac.2016.02.027
7. Shipley, H.J., Engates, K.E., Grover, V.A., Environ. Sci. Pollut. Res. 20, 1727-1736 (2013) https://doi.org/10.1007/s11356-012-0984-z
8. Van Turan, C., Quang, D.V., Nguyen Thi, H.P.: Truong, T.N.; La, D.D., ACS Omga, 5, 7298-7306 (2020) https://doi.org/10.1021/acsomega.9b04126
9. Homayonfard, A., Miralinaghi, M., Haji Seyed Mohammad Shirazi, R., Moniri, E., Water Sci. Technol. 78, 2297-2307 (2018) https://doi.org/10.2166/wst.2018.510
10. Fu, F., Wang, Q., J. Environ. Manag. 92, 407-418 (2011) https://doi.org/10.1016/j.jenvman.2010.11.011
11. Zhang, H., Xu, F., Xue, J., Chen, S., Wang, J., Yang, Y., Sci. Rep. 10, Article number: 6067 (2020) https://doi.org/10.1038/s41598-020-63000-z
12. Malik, L.A., Bashir, A., Qureashi, A., Pandith, A.H., Environ. Chem. Lett. 17, 1495-1521 (2019) https://doi.org/10.1007/s10311-019-00891-z
13. Bashir, A., Malik, L.A., Ahad, S., Manzoor, T., Bhat, M.A., Dar, G.N., Pandith, A.H., Environ. Chem. Lett. 17, 729-754 (2019) https://doi.org/10.1007/s10311-018-00828-y
14. Shayegan, H., Ali, G.A.M., Safarifard, V., ChemSelect. 5, 124-146 (2020) https://doi.org/10.1002/slct.201904107
15. Zhang, C., Su, J., Zhu, H., Xiong, J., Liu, X., Li, D., Chen, Y., Li, Y., RSC Adv. 7, 34182-34191 (2017) https://doi.org/10.1039/C7RA03056H
16. Alalwan, H.A., Kadhom, M.A., Alminshid, A.H., J. Water Supp. Res. Technol. Aqua 69, 99-112 (2020) https://doi.org/10.2166/aqua.2020.133
17. Aklil, A., Mouflih, M., Sebti, S., J. Hazard. Mater. 112, 183-190 (2004) https://doi.org/10.1016/j.jhazmat.2004.05.018
18. Kul, A.R., Koyuncu, H., J. Hazard. Mater. 179, 332-339 (2010) https://doi.org/10.1016/j.jhazmat.2010.03.009
19. Zou, C., Jiang, W., Liang, J., Sun, X., Guan, Y., Environ. Sci. Pollut. Res. 26, 1315-1322 (2019) https://doi.org/10.1007/s11356-018-3652-0
20. Yao, O., Xie, J., Liu, J., Kang, H., Liu, Y., J. Polym. Res. 21, 465 (2014) https://doi.org/10.1007/s10965-014-0465-9
21. Nurain Ahmad, S.Z., Wan Salleh, W.N., Yusof, N., Mohd Yusop, M.Z., Hamdan, R., Awang, N.A., Ismail, N.H., Rosman, N., Sazali, N., Fauzi Ismail, A., Chem. Eng. Commun. 208, 646-660 (2021) https://doi.org/10.1080/00986445.2020.1715957
22. Palma-Anaya, E., Fall, C., Torres-Blancas, T., Balderas-Hernández, P., Cruz-Olivares, J., Barrera-Díaz, C.E., Roa-Morales, G., J. Chem. 8, Article ID 4296515 (2017) https://doi.org/10.1155/2017/4296515
23. Abdolahpour, S., Farrokhnia, A., Abbasi, Z., Iran. J. Chem. Chem. Eng. 38, 155-163 (2019)
24. Raji, F., Saraeian, A., Pakizeh, M., Attarzadeh, F., RSC Adv. 5, 37066-37077 (2015) https://doi.org/10.1039/C5RA01192B
25. Rahdar, S., Rahdar, A., Sattari, M., Divband Hafshejani, L., Tolkou, A.K., Kyzas, G.Z., Polymers 13, 1161 (2021) https://doi.org/10.3390/polym13071161
26. Gutiérrez-López, D., Flores-Alamo, N., Carreño-de-León, M. C., Solache-Rios, M. J., Water Supp. 20, 2133-2144 (2020) https://doi.org/10.2166/ws.2020.107
27. Xu, X., Hao, R., Xu, H., Lu, A., Sci. Rep. 10, 9079 (2020) https://doi.org/10.1038/s41598-020-66025-6
28. Rahdar, A., Rahdar, S., Labuto, G., Environ. Sci. Pollut. Res. Int. 27, 9181-9191 (2020) https://doi.org/10.1007/s11356-019-07491-y
29. Tamez, C., Hernandez, R., Parsons, J.G., Microchem. J. 125, 97-104 (2016) https://doi.org/10.1016/j.microc.2015.10.028
30. Cao, C.Y., Qu, J., Yan, W.S., Zhu, J.F., Wu, Z.Y., Song, W.G., Langmuir 28, 4573-4579 (2012) https://doi.org/10.1021/la300097y
31. Tsedenbal, B., Lee, J.E., Huh, S.H., Koo, B.H., Lee, C.G., Korean J. Mater. Res. 30, 447452 (2020). https://doi.org/10.3740/MRSK.2020.30.9.447
32. Jerin, V.M., Remya, R., Thomas, M., Varkey, J.T., Mater. Today Proceed. 9, 27-31 (2019). https://doi.org/10.1016/j.matpr.2019.02.032
33. Khosravi, M., Azizian, S., J. Indust. Eng. Chem. 20, 2561-2567 (2014). https://doi.org/10.1016/j.jiec.2013.10.040
34. Debnath, A., Deb, K., Chattopadhyay, K.K., Saha, B., Desalin. Water Treat. 57, 13549-13560 (2016). https://doi.org/10.1080/19443994.2015.1060540
35. Kusior, A., Michalec, K., Jelen, P., Radecka, M., App. Surface Sci. 476, 342-352 (2019). https://doi.org/10.1016/j.apsusc.2018.12.113
36. Ye, C., Hu, K., Niu, Z., Lu, Y., Zhang, L., Yan, K., J. Water Process Eng. 27, 205-210 (2019). https://doi.org/10.1016/j.jwpe.2018.12.008
37. Khalaji, A.D., Palang Sangdevini, Z., Mousavi, S.M., Jarosova, M., Machek, P., Asian J. Nanosci. Mater. 4, 137-146 (2021)
38. Khalaji, A.D., Ghorbani, M., Chem. Method. 4, 532-542 (2020) https://doi.org/10.33945/SAMI/CHEMM.2020.4.12
39. Khalaji, A.D., Chem. Method. 3, 635-643 (2019) https://doi.org/10.33945/SAMI/CHEMM.2019.5.6
40. Khalaji, A.D., Asian J. Nanosci. Mater. 2, 186-190 (2019)
41. Khalaji, A.D., Grivani, G., Izadi, S., Ebadi, M., J. Nanoanalysis 5, 115-120 (2018)

42. Khalaji, A.D., Mousavi, S.M., Jarosova, M., Machek, P., J. Surface Invest. X-ray. Synch. Neut. Tech. 14, 1191-1194 (2020) https://doi.org/10.1134/S1027451020060051
43. Petricek, V., Dusek, M., Palatinus, L., Z. Kristallogr. 229, 345-352 (2004) https://doi.org/10.1515/zkri-2014-1737
44. Williamson, G.K., Hall, W.H., Acta Metall. 1, 22-31 (1953) https://doi.org/10.1016/0001-6160(53)90006-6
45. Cheary, R.W., Coelho, A.A., J. Appl. Cryst. 31, 862-868 (1998) https://doi.org/10.1107/S0021889898006888
46. Zak, A.K., Abd Majid, W.H., Abrishami, M.E., Yousefi, R., Solid State Sci. 13, 251-256 (2011) https://doi.org/10.1016/j.solidstatesciences.2010.11.024
47. Dave, P.N., Chopda, L.V., J. Nanotechnol. Article ID 398569, 14 pages (2014) https://doi.org/10.1155/2014/398569
48. Yuvaraja, G., Pang, Y., Chen, D.Y., Kong, L.J., Mehmood, S., Subbaiah, M.V., Rao, D.S., Pavuluri, C.M., Wen, J.C., Reddy, G.M., Int. J. Biol. Macromol. 136, 177-188 (2019) https://doi.org/10.1016/j.ijbiomac.2019.06.016
49. Weijiang, Z., Yace, Z., Yuvaraja, G., Jiao, X., Int. J. Biol. Macromol. 105, 422-430 (2017) https://doi.org/10.1016/j.ijbiomac.2017.07.063
50. Yan, Y., Yuvaraja, G., Liu, C., Kong, L., Guo, K., Reddy, G.M., Zyryanov, G.V., Int. J. Biol. Macromol. 117, 1305-1313 (2018) https://doi.org/10.1016/j.ijbiomac.2018.05.204
51. Hussain, M.S., Musharraf, S.G., Bhanger, M.I., Malik, M.I., Int. J. Biol. Macromol. 147, 643-652 (2020) https://doi.org/10.1016/j.ijbiomac.2020.01.091
52. Yuvaraja, G., Subbaiah, M.V., Int. J. Biol. Macromol. 93, 408-417 (2016)
53. Shahraki, S., Delarami, H.S., Khosravi, F., Int. J. Biol. Macromol. 139, 577-586 (2019). https://doi.org/10.1016/j.ijbiomac.2019.07.223